

Tri-Hexagonal charge order in kagome metal CsV_3Sb_5 revealed by ^{121}Sb NQR

Chao Mu,^{1,2} Qiangwei Yin,³ Zhijun Tu,³ Chunsheng Gong,³
Ping Zheng,¹ Hechang Lei,^{3,*} Zheng Li,^{1,2,†} and Jianlin Luo^{1,2,4}

¹*Beijing National Laboratory for Condensed Matter Physics and Institute of Physics,
Chinese Academy of Sciences, Beijing 100190, China*

²*School of Physical Sciences, University of Chinese Academy of Sciences, Beijing 100190, China*

³*Department of Physics and Beijing Key Laboratory of Opto-electronic Functional Materials & Micro-nano Devices,
Renmin University of China, Beijing 100872, China*

⁴*Songshan Lake Materials Laboratory, Dongguan 523808, China*

We report ^{121}Sb nuclear quadrupole resonance (NQR) measurements on kagome superconductor CsV_3Sb_5 with $T_c = 2.5$ K. ^{121}Sb NQR spectra split after a charge density wave (CDW) transition at 94 K, which demonstrates a commensurate CDW state. The coexistence of the high temperature phase and the CDW phase between 91 K and 94 K manifests that it is a first order phase transition. The CDW order exhibits Tri-Hexagonal deformation with a lateral shift between the adjacent kagome layers, which is consistent with $2 \times 2 \times 2$ superlattice modulation. The superconducting state coexists with CDW order and shows a conventional s-wave behavior in the bulk state.

PACS numbers: 74.25.nj, 71.45.Lr, 76.60.Gv, 76.60.-k

The newly discovered superconductor AV_3Sb_5 ($A = \text{K, Rb, Cs}$) possesses a quasi-two-dimensional kagome structure, which provides a platform to investigate the interplay of topology, electron correlation effects and superconductivity[1–5]. They undergo a charge density wave (CDW) transition at $T_{\text{CDW}} = 78$ K, 103 K, 94 K and a superconducting transition at $T_c = 0.93$ K, 0.92 K, and 2.5 K for $A = \text{K, Rb, Cs}$, respectively. The superconducting state is found to be spin singlet with s-wave pairing symmetry in the bulk state[6–8]. STM studies observed possible Majorana modes[9] and pair density wave[10] in the surface state. There are also experimentally observed residual density of states in the superconducting state[11], which may be due to the competition between the superconductivity and the CDW[11–16].

The CDW order breaks time-reversal symmetry[17–19] and leads to the anomalous Hall effect in the absence of magnetic local moments[20–23]. Inelastic x-ray scattering and Raman scattering exclude strong electron-phonon coupling driven CDW[24], while optical spectroscopy supports CDW is driven by nesting of Fermi surfaces[25]. STM experiment found the CDW peak intensities at $3Q$ which breaks six-fold rotational symmetry[26]. An additional unidirectional 1×4 superlattice is observed on the surface[10, 27–29], but is absent in the bulk state[30]. The “Star of David” (SoD) and “Tri-Hexagonal” (TrH) structure configurations are proposed to be the likely candidates for CDW structures[31, 32], as illustrated in Fig.2(b) and (c). SoD or TrH with a lateral shift between the adjacent Kagome layer results in a $2 \times 2 \times 2$ structure modulation[33]. Density functional theory calculations show that the TrH deformation is preferred[31, 32, 34]. However, there is still lack experimental evidence whether SoD or TrH defor-

mation is the ground state configuration in the CDW state.

In this work, we report nuclear quadrupole resonance (NQR) investigations on CsV_3Sb_5 . The splitting of ^{121}Sb spectra demonstrates that a commensurate CDW order forms at 94 K with a first-order transition. Our results indicate that the charge order has a Tri-Hexagonal deformation which is 2×2 period modulation. The shift between the adjacent kagome layers induces a modulation in the c -direction and the CDW is a three-dimensional modulation with $2 \times 2 \times 2$ period. Spin-lattice relaxation rate measured at the peak of the CDW state shows a coherence peak just below T_c , indicating that the superconducting state coexists with the CDW order and shows a conventional s-wave behavior.

Single crystals of CsV_3Sb_5 were synthesized using the self-flux method[6]. Superconductivity with $T_c = 2.5$ K is confirmed by dc magnetization measured using a superconducting quantum interference device (SQUID). The NQR measurements were performed using a phase coherent spectrometer. The spectra were obtained by frequency step and sum method which sums the Fourier transformed spectra at a series of frequencies[35]. The spin-lattice relaxation time T_1 was measured using a single saturation pulse. Crystal structures were visualized in VESTA[36].

Figure 1 shows the NQR spectra of ^{121}Sb in zero field. There are two different crystallographic sites of Sb in CsV_3Sb_5 with the atomic ratio of $\text{Sb1} : \text{Sb2} = 1 : 4$. Sb1 is located in the V-kagome plane, and Sb2 forms a graphite-like network between V-kagome layers, as shown in the inset of Fig. 1 and Fig. 2 (a). It is easy to distinguish Sb2 peaks from Sb1 peaks by the spectral intensity. The nuclear spin Hamiltonian of the interaction between quadrupole moment Q and the electric field gradient (EFG) is described as

$$\mathcal{H}_Q = \frac{h\nu_Q}{6} \left[(3I_z^2 - I^2) + \frac{\eta}{2}(I_+^2 + I_-^2) \right] \quad (1)$$

* hlei@ruc.edu.cn

† lizheng@iphy.ac.cn

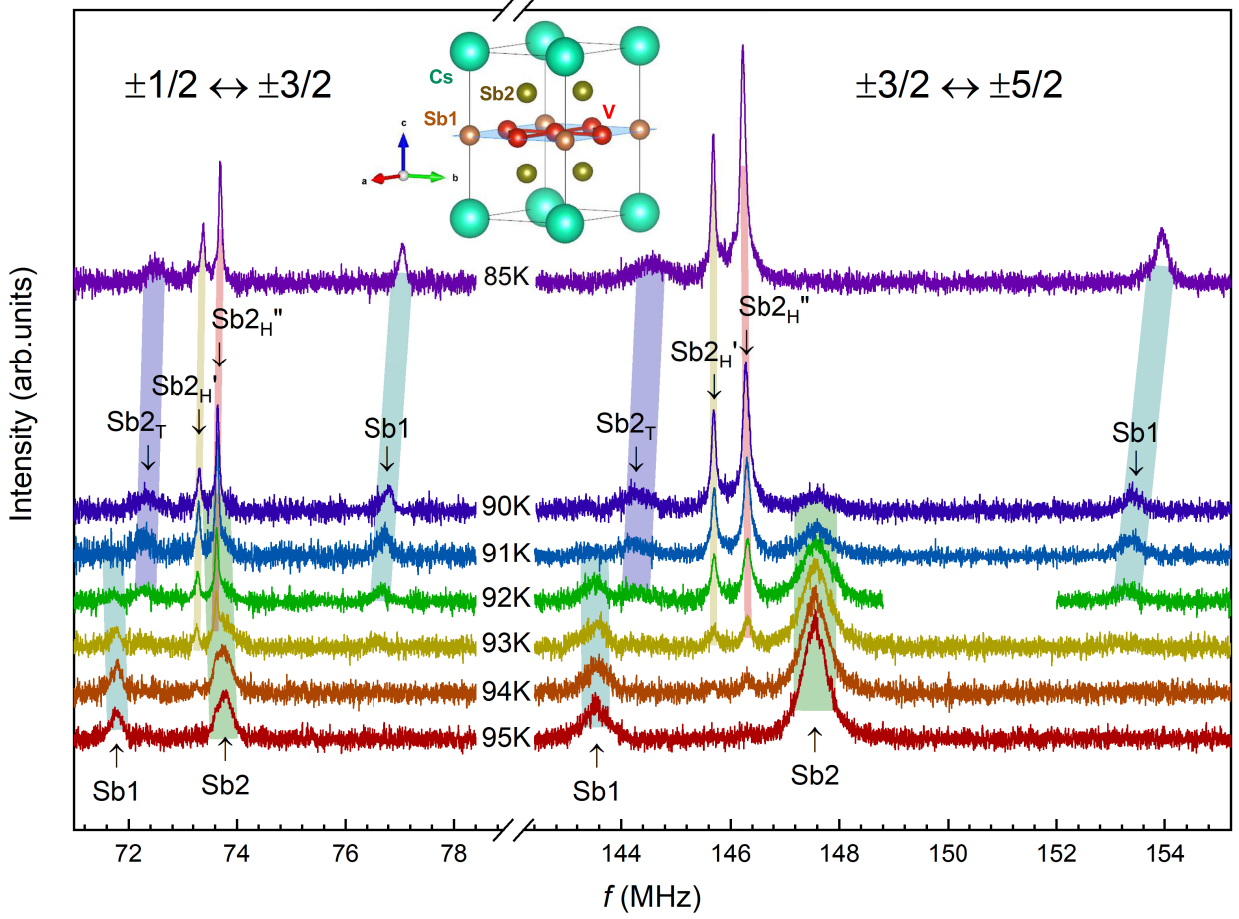


FIG. 1. ^{121}Sb -NQR spectra around T_{CDW} . The peaks in the low frequency range are from $\pm\frac{1}{2} \leftrightarrow \pm\frac{3}{2}$ transition and the peaks in the high frequency range are from $\pm\frac{3}{2} \leftrightarrow \pm\frac{5}{2}$ transition. There are 2 sites of Sb marked by Sb1 and Sb2 above T_{CDW} . Both peaks of Sb2 split due to non-equivalent sites emerge below T_{CDW} . The notations of Sb1, Sb2_H, Sb2'_H and Sb2_T are consistent with Fig. 2(c). The spectra of all temperatures are presented in the supplemental material.

where ν_Q is the quadrupole resonance frequency along the principal axis (c -axis), $\nu_Q \equiv \frac{3e^2qQ}{2I(2I-1)}$, with $eq = V_{zz}$. η is an asymmetry parameter of the EFG, $\eta = \frac{V_{xx} - V_{yy}}{V_{zz}}$, where V_{xx} , V_{yy} , V_{zz} are the EFGs along the x , y , z directions respectively. ^{121}Sb with $I = 5/2$ has two NQR peaks for each site, $|\pm\frac{1}{2}\rangle \leftrightarrow |\pm\frac{3}{2}\rangle$ transition at low frequency and $|\pm\frac{3}{2}\rangle \leftrightarrow |\pm\frac{5}{2}\rangle$ transition at high frequency.

Four NQR transition peaks can be clearly identified above 95 K. Below $T_{\text{CDW}} = 94$ K, the intensity of original peaks decreases gradually and four sets of new peaks emerge, indicating that the CDW transition is commensurate and four unequal sites of Sb atoms appear in the CDW state. The coexistence of two phases between 91 K and 94 K demonstrates that the CDW transition is of first-order due to a simultaneous superlattice transition[2]. It is consistent with NMR studies on ^{51}V which also show coexistent behavior[6, 37, 38]. The peaks below T_{CDW} are complex and cannot be distinguished by intensity alone.

Two structure configurations named as “Star of David”

and “Tri-Hexagonal” have been proposed in the CDW state[31, 32, 34]. We can assign the Sb2_H and Sb2_T sites by their symmetry. In SoD configuration, as shown in Fig. 2 (b), Sb2_H is inside the star and Sb2_T is outside the star. In TrH configuration, as shown in Fig. 2 (c), Sb2_T is located at the center of the trigonal V-network and Sb2_H is outside. A lateral shift between the adjacent kagome layer form modulation on the c -axis[33, 34], which result in a nematic state with only C_2 rotation symmetry and make Sb2'_H site different from Sb2''_H site[39]. The subscript of “H” denotes the sites around the hexagon and the subscript of “T” denotes the sites at the triangle center. The four new peaks in Fig. 1 correspond to these four sites, Sb1, Sb2'_H, Sb2''_H and Sb2_T. The spin-lattice relaxation time, T_1 , is employed to track the evolution of the peaks. $1/T_1T$ of the peak around 77 MHz evolves from Sb1, as shown in Fig. 3. $1/T_1T$ of the peaks around 74 MHz marked by Sb2'_H and Sb2''_H are same and evolve from Sb2, see the Fig. 2 in Ref [6]. The peak around 72 MHz has weak intensity and T_1 measurement has large uncertainty just below T_{CDW} . Fortunately, there is only

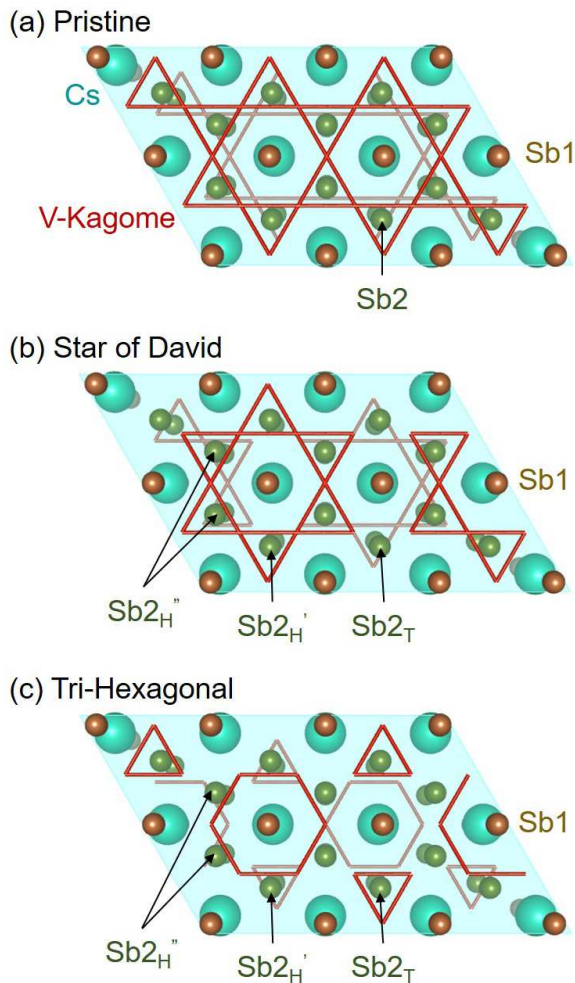


FIG. 2. Perspective view of crystal structures of CsV_3Sb_5 in (a) the pristine phase, (b) the star of David phase and (c) the Tri-hexagonal phase. There is a shift between adjacent layer in the star of David configuration and the Tri-hexagonal configuration.

$\text{Sb}_{2\text{T}}$ site left, so the peak around 72 MHz is attributed to it. In addition, the asymmetry parameters η can also be used to distinguish them.

All peak positions are summarized in Fig. 4 (a)(d). Combining the frequencies of $|\pm \frac{1}{2}\rangle \leftrightarrow |\pm \frac{3}{2}\rangle$ transition and $|\pm \frac{3}{2}\rangle \leftrightarrow |\pm \frac{5}{2}\rangle$ transition, ν_Q and η are calculated, as shown in Fig. 4(b)(c)(e)(f). The η at all sites is zero above T_{CDW} , reflecting the isotropy of EFG in the xy -plane. Below T_{CDW} , η of Sb2 changes to finite values, indicating the in-plane symmetry is broken and unequal sites of Sb2 are generated. The slightly decreasing ν_Q implies that the main change is not the EFG strength, but the EFG direction at Sb2 sites. On the other hand, Sb1 in kagome plane has high symmetry, so the EFG at Sb1 site changes frequency obviously without asymmetry. When the electric field modulation period is twice the lattice constant, the highly symmetrical sites are not

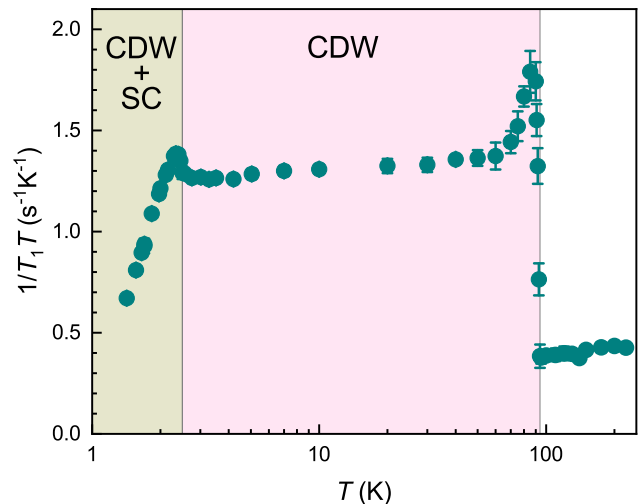


FIG. 3. Temperature dependence of $^{121}(1/T_1T)$ of Sb1 site. $1/T_1T$ jumps at T_{CDW} . A Hebel-Slichter coherence peak appears just below T_c .

affected by the modulation[40], so Sb1 peak does not split like Sb2 peak.

Next, we will distinguish between the two configurations of TrH and SoD. The CDW has a three-dimensional modulation and the modulation in c -axis will make Sb2 plane has different pattern from the kagome plane. Therefore, the different between TrH and SoD in the kagome plane should be detected by Sb1 rather than Sb2. In TrH deformation, V atoms are closer to Sb1 site, so ν_Q of Sb1 moves a lot toward high frequency, as shown in Fig. 4 (b). In SoD deformation, on the other hand, V atoms move away from Sb1 site, so ν_Q of Sb1 should not increase, which is inconsistent with the NQR spectra. The $\text{Sb}_{2\text{H}}$ peaks split to $\text{Sb}_{2\text{H}'}$ and $\text{Sb}_{2\text{H}''}$ peaks due to a lateral shift between adjacent layer in the Tri-hexagonal configuration. The intensity ratio of two peaks are 1 : 2, which is consistent with the atoms ratio. NQR frequency is determined by EFG, so the NQR spectra indicates that the electronic modulation pattern is formed simultaneously with the structural distortion. Our results favor TrH deformation over SoD deformation and are consistent with $2a \times 2a \times 2c$ pattern. If $4a$ pattern exists, it should only exist on the surface[30, 32].

ν_Q and η jump at T_{CDW} and then change gradually in the CDW state. They remain constant when entering the superconducting state, indicating the coexistence of superconductivity and the CDW order. $^{121}(1/T_1T)$ measured at the peak in the CDW order state shows superconducting transition, as shown in Fig. 3, confirming the coexistence. $^{121}(1/T_1T)$ shows a clear Hebel-Slichter coherence peak just below T_c and then rapidly decreases at low temperatures, as shown in Fig. 3, indicating that CsV_3Sb_5 is a conventional s-wave superconductor. It is consistent with our previous result measured at Sb2 site[6].

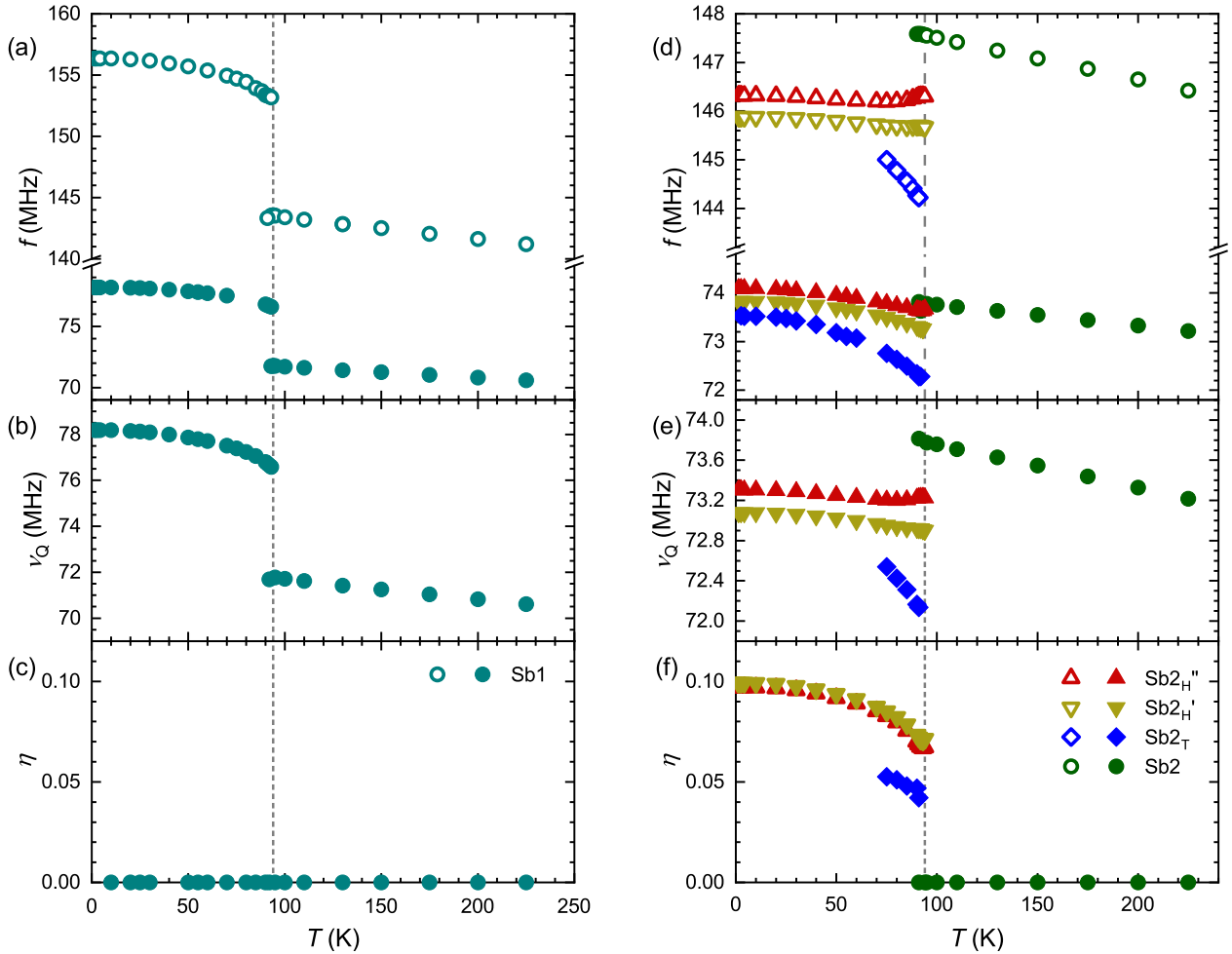


FIG. 4. Temperature dependence of (a)(d) peak positions, (b)(e) ν_Q and (f)(g) η of Sb1 site and Sb2 site, respectively. The vertical dashed lines indicate the transition temperature of CDW.

In conclusion, we have performed ^{121}Sb NQR studies on CsV_3Sb_5 . The variation of the NQR spectra indicates a first-order commensurate CDW transition occurs at 94 K. We identified four Sb sites in the CDW state which give restriction on the CDW order. The charge order can be understood in terms of Tri-Hexagonal deformation with lateral shift between the adjacent kagome layers, which has a $2 \times 2 \times 2$ period. In the superconducting state, $^{121}(1/T_1T)$ of Sb1 site in kagome planes shows conventional s-wave behavior, just as $^{121}(1/T_1T)$ of Sb2 site between kagome planes. The superconducting

phase coexist with CDW order in the bulk state.

This work was supported by the National Key Research and Development Program of China (Grant No. 2017YFA0302901, 2018YFA0305702, 2018YFE0202600, and 2016YFA0300504), the National Natural Science Foundation of China (Grant No. 12134018, 11921004, 11822412 and 11774423), the Beijing Natural Science Foundation (Grant No. Z200005), and the Strategic Priority Research Program and Key Research Program of Frontier Sciences of the Chinese Academy of Sciences (Grant No. XDB33010100).

[1] B. R. Ortiz, L. C. Gomes, J. R. Morey, M. Winiarski, M. Bordelon, J. S. Mangum, I. W. H. Oswald, J. A. Rodriguez-Rivera, J. R. Neilson, S. D. Wilson, E. Ertekin, T. M. McQueen, and E. S. Toberer, New kagome prototype materials: discovery of KV_3Sb_5 , RbV_3Sb_5 , and CsV_3Sb_5 , *Phys. Rev. Materials* **3**, 094407 (2019).

[2] B. R. Ortiz, S. M. L. Teicher, Y. Hu, J. L. Zuo, P. M. Sarte, E. C. Schueller, A. M. M. Abeykoon, M. J. Krogstad, S. Rosenkranz, R. Osborn, R. Seshadri, L. Balents, J. He, and S. D. Wilson, CsV_3Sb_5 : A Z_2 Topological Kagome Metal with a Superconducting Ground State, *Phys. Rev. Lett.* **125**, 247002 (2020).

[3] B. R. Ortiz, P. M. Sarte, E. M. Kenney, M. J. Graf,

- S. M. L. Teicher, R. Seshadri, and S. D. Wilson, Superconductivity in the \mathbb{Z}_2 kagome metal KV_3Sb_5 , *Phys. Rev. Materials* **5**, 034801 (2021).
- [4] Q. W. Yin, Z. J. Tu, C. S. Gong, Y. Fu, S. H. Yan, and H. C. Lei, Superconductivity and Normal-State Properties of Kagome Metal RbV_3Sb_5 Single Crystals, *Chinese Physics Letters* **38**, 6 (2021).
- [5] K. Jiang, T. Wu, J.-X. Yin, Z. Wang, M. Z. Hasan, S. D. Wilson, X. Chen, and J. Hu, Kagome superconductors AV_3Sb_5 ($A=K, Rb, Cs$) (2021), arXiv:2109.10809 [cond-mat.supr-con].
- [6] C. Mu, Q. Yin, Z. Tu, C. Gong, H. Lei, Z. Li, and J. Luo, S-Wave Superconductivity in Kagome Metal CsV_3Sb_5 Revealed by $^{121/123}Sb$ NQR and ^{51}V NMR Measurements, *Chinese Physics Letters* **38**, 077402 (2021).
- [7] H.-S. Xu, Y.-J. Yan, R. Yin, W. Xia, S. Fang, Z. Chen, Y. Li, W. Yang, Y. Guo, and D.-L. Feng, Multiband Superconductivity with Sign-Preserving Order Parameter in Kagome Superconductor CsV_3Sb_5 , *Phys. Rev. Lett.* **127**, 187004 (2021).
- [8] W. Duan, Z. Nie, S. Luo, F. Yu, B. R. Ortiz, L. Yin, H. Su, F. Du, A. Wang, Y. Chen, X. Lu, J. Ying, S. D. Wilson, X. Chen, Y. Song, and H. Yuan, Nodeless superconductivity in the kagome metal CsV_3Sb_5 , *Science China Physics, Mechanics & Astronomy* **64**, 107462 (2021).
- [9] Z. Liang, X. Hou, F. Zhang, W. Ma, P. Wu, Z. Zhang, F. Yu, J.-J. Ying, K. Jiang, L. Shan, Z. Wang, and X.-H. Chen, Three-Dimensional Charge Density Wave and Surface-Dependent Vortex-Core States in a Kagome Superconductor CsV_3Sb_5 , *Phys. Rev. X* **11**, 031026 (2021).
- [10] H. Chen, H. Yang, B. Hu, Z. Zhao, J. Yuan, Y. Xing, G. Qian, Z. Huang, G. Li, Y. Ye, S. Ma, S. Ni, H. Zhang, Q. Yin, C. Gong, Z. Tu, H. Lei, H. Tan, S. Zhou, C. Shen, X. Dong, B. Yan, Z. Wang, and H.-J. Gao, Roton pair density wave in a strong-coupling kagome superconductor, *Nature* 10.1038/s41586-021-03983-5 (2021).
- [11] C. C. Zhao, L. S. Wang, W. Xia, Q. W. Yin, J. M. Ni, Y. Y. Huang, C. P. Tu, Z. C. Tao, Z. J. Tu, C. S. Gong, H. C. Lei, Y. F. Guo, X. F. Yang, and S. Y. Li, Nodal superconductivity and superconducting domes in the topological Kagome metal CsV_3Sb_5 (2021), arXiv:2102.08356 [cond-mat.supr-con].
- [12] K. Y. Chen, N. N. Wang, Q. W. Yin, Y. H. Gu, K. Jiang, Z. J. Tu, C. S. Gong, Y. Uwatoko, J. P. Sun, H. C. Lei, J. P. Hu, and J.-G. Cheng, Double Superconducting Dome and Triple Enhancement of T_c in the Kagome Superconductor CsV_3Sb_5 under High Pressure, *Phys. Rev. Lett.* **126**, 247001 (2021).
- [13] F. H. Yu, D. H. Ma, W. Z. Zhuo, S. Q. Liu, X. K. Wen, B. Lei, J. J. Ying, and X. H. Chen, Unusual competition of superconductivity and charge-density-wave state in a compressed topological kagome metal, *Nature Communications* **12**, 3645 (2021).
- [14] F. Du, S. Luo, B. R. Ortiz, Y. Chen, W. Duan, D. Zhang, X. Lu, S. D. Wilson, Y. Song, and H. Yuan, Pressure-induced double superconducting domes and charge instability in the kagome metal KV_3Sb_5 , *Phys. Rev. B* **103**, L220504 (2021).
- [15] Z. Zhang, Z. Chen, Y. Zhou, Y. Yuan, S. Wang, J. Wang, H. Yang, C. An, L. Zhang, X. Zhu, Y. Zhou, X. Chen, J. Zhou, and Z. Yang, Pressure-induced reemergence of superconductivity in the topological kagome metal CsV_3Sb_5 , *Phys. Rev. B* **103**, 224513 (2021).
- [16] X. Chen, X. Zhan, X. Wang, J. Deng, X.-B. Liu, X. Chen, J.-G. Guo, and X. Chen, Highly Robust Reentrant Superconductivity in CsV_3Sb_5 under Pressure, *Chinese Physics Letters* **38**, 057402 (2021).
- [17] Y.-X. Jiang, J.-X. Yin, M. M. Denner, N. Shumiya, B. R. Ortiz, G. Xu, Z. Guguchia, J. He, M. S. Hossain, X. Liu, J. Ruff, L. Kautzsch, S. S. Zhang, G. Chang, I. Belopolski, Q. Zhang, T. A. Cochran, D. Multer, M. Litskevich, Z.-J. Cheng, X. P. Yang, Z. Wang, R. Thomale, T. Neupert, S. D. Wilson, and M. Z. Hasan, Unconventional chiral charge order in kagome superconductor KV_3Sb_5 , *Nature Materials* **20**, 1353 (2021).
- [18] N. Shumiya, M. S. Hossain, J.-X. Yin, Y.-X. Jiang, B. R. Ortiz, H. Liu, Y. Shi, Q. Yin, H. Lei, S. S. Zhang, G. Chang, Q. Zhang, T. A. Cochran, D. Multer, M. Litskevich, Z.-J. Cheng, X. P. Yang, Z. Guguchia, S. D. Wilson, and M. Z. Hasan, Intrinsic nature of chiral charge order in the kagome superconductor RbV_3Sb_5 , *Phys. Rev. B* **104**, 035131 (2021).
- [19] C. M. III, D. Das, J. X. Yin, H. Liu, R. Gupta, C. N. Wang, Y. X. Jiang, M. Medarde, X. Wu, H. C. Lei, J. J. Chang, P. Dai, Q. Si, H. Miao, R. Thomale, T. Neupert, Y. Shi, R. Khasanov, M. Z. Hasan, H. Luetkens, and Z. Guguchia, Time-reversal symmetry-breaking charge order in a correlated kagome superconductor (2021), arXiv:2106.13443 [cond-mat.mtrl-sci].
- [20] S.-Y. Yang, Y. Wang, B. R. Ortiz, D. Liu, J. Gayles, E. Derunova, R. Gonzalez-Hernandez, L. Šmejkal, Y. Chen, S. S. P. Parkin, S. D. Wilson, E. S. Toberer, T. McQueen, and M. N. Ali, Giant, unconventional anomalous Hall effect in the metallic frustrated magnet candidate, KV_3Sb_5 , *Science Advances* **6**, eabb6003 (2020).
- [21] E. M. Kenney, B. R. Ortiz, C. Wang, S. D. Wilson, and M. J. Graf, Absence of local moments in the kagome metal KV_3Sb_5 as determined by muon spin spectroscopy, *Journal of Physics: Condensed Matter* **33**, 235801 (2021).
- [22] F. H. Yu, T. Wu, Z. Y. Wang, B. Lei, W. Z. Zhuo, J. J. Ying, and X. H. Chen, Coexistence of anomalous Hall effect and charge density wave in a superconducting topological kagome metal, *Phys. Rev. B* **104**, L041103 (2021).
- [23] X. Feng, K. Jiang, Z. Wang, and J. Hu, Chiral flux phase in the Kagome superconductor AV_3Sb_5 , *Science Bulletin* **66**, 1384 (2021).
- [24] H. Li, T. T. Zhang, T. Yilmaz, Y. Y. Pai, C. E. Marviny, A. Said, Q. W. Yin, C. S. Gong, Z. J. Tu, E. Vescovo, C. S. Nelson, R. G. Moore, S. Murakami, H. C. Lei, H. N. Lee, B. J. Lawrie, and H. Miao, Observation of Unconventional Charge Density Wave without Acoustic Phonon Anomaly in Kagome Superconductors AV_3Sb_5 ($A = Rb, Cs$), *Phys. Rev. X* **11**, 031050 (2021).
- [25] X. Zhou, Y. Li, X. Fan, J. Hao, Y. Dai, Z. Wang, Y. Yao, and H.-H. Wen, Origin of charge density wave in the kagome metal CsV_3Sb_5 as revealed by optical spectroscopy, *Phys. Rev. B* **104**, L041101 (2021).
- [26] Y.-X. Jiang, J.-X. Yin, M. M. Denner, N. Shumiya, B. R. Ortiz, G. Xu, Z. Guguchia, J. He, M. S. Hossain, X. Liu, J. Ruff, L. Kautzsch, S. S. Zhang, G. Chang, I. Belopolski, Q. Zhang, T. A. Cochran, D. Multer, M. Litskevich, Z.-J. Cheng, X. P. Yang, Z. Wang, R. Thomale, T. Neupert, S. D. Wilson, and M. Z. Hasan, Unconventional chiral charge order in kagome superconductor KV_3Sb_5 , *Nature Materials* **20**, 1353 (2021).

- [27] H. Zhao, H. Li, B. R. Ortiz, S. M. L. Teicher, T. Park, M. Ye, Z. Wang, L. Balents, S. D. Wilson, and I. Zeljkovic, Cascade of correlated electron states in a kagome superconductor CsV_3Sb_5 , *Nature* 10.1038/s41586-021-03946-w (2021).
- [28] Z. Liang, X. Hou, F. Zhang, W. Ma, P. Wu, Z. Zhang, F. Yu, J.-J. Ying, K. Jiang, L. Shan, Z. Wang, and X.-H. Chen, Three-Dimensional Charge Density Wave and Surface-Dependent Vortex-Core States in a Kagome Superconductor CsV_3Sb_5 , *Phys. Rev. X* **11**, 031026 (2021).
- [29] Z. Wang, Y.-X. Jiang, J.-X. Yin, Y. Li, G.-Y. Wang, H.-L. Huang, S. Shao, J. Liu, P. Zhu, N. Shumiya, M. S. Hossain, H. Liu, Y. Shi, J. Duan, X. Li, G. Chang, P. Dai, Z. Ye, G. Xu, Y. Wang, H. Zheng, J. Jia, M. Z. Hasan, and Y. Yao, Electronic nature of chiral charge order in the kagome superconductor CsV_3Sb_5 , *Phys. Rev. B* **104**, 075148 (2021).
- [30] H. Li, Y.-X. Jiang, J. X. Yin, S. Yoon, A. R. Lupini, Y. Pai, C. Nelson, A. Said, Y. M. Yang, Q. W. Yin, C. S. Gong, Z. J. Tu, H. C. Lei, B. Yan, Z. Wang, M. Z. Hasan, H. N. Lee, and H. Miao, Spatial symmetry constraint of charge-ordered kagome superconductor CsV_3Sb_5 (2021), arXiv:2109.03418 [cond-mat.mtrl-sci].
- [31] B. R. Ortiz, S. M. L. Teicher, L. Kautzsch, P. M. Sarte, N. Ratcliff, J. Harter, J. P. C. Ruff, R. Seshadri, and S. D. Wilson, Fermi surface mapping and the nature of charge-density-wave order in the kagome superconductor CsV_3Sb_5 , *Phys. Rev. X* **11**, 041030 (2021).
- [32] H. Tan, Y. Liu, Z. Wang, and B. Yan, Charge density waves and electronic properties of superconducting kagome metals, *Phys. Rev. Lett.* **127**, 046401 (2021).
- [33] H. Miao, H. X. Li, W. R. Meier, A. Huon, H. N. Lee, A. Said, H. C. Lei, B. R. Ortiz, S. D. Wilson, J. X. Yin, M. Z. Hasan, Z. Wang, H. Tan, and B. Yan, Geometry of the charge density wave in the kagome metal AV_3Sb_5 , *Phys. Rev. B* **104**, 195132 (2021).
- [34] N. Ratcliff, L. Hallett, B. R. Ortiz, S. D. Wilson, and J. W. Harter, Coherent phonon spectroscopy and interlayer modulation of charge density wave order in the kagome metal CsV_3Sb_5 , *Phys. Rev. Materials* **5**, L111801 (2021).
- [35] W. G. Clark, M. E. Hanson, F. Lefloch, and P. Ségransan, Magnetic resonance spectral reconstruction using frequency-shifted and summed Fourier transform processing, *Review of Scientific Instruments* **66**, 2453 (1995).
- [36] K. Momma and F. Izumi, *VESTA3* for three-dimensional visualization of crystal, volumetric and morphology data, *Journal of Applied Crystallography* **44**, 1272 (2011).
- [37] D. W. Song, L. X. Zheng, F. H. Yu, J. Li, L. P. Nie, M. Shan, D. Zhao, S. J. Li, B. L. Kang, Z. M. Wu, Y. B. Zhou, K. L. Sun, K. Liu, X. G. Luo, Z. Y. Wang, J. J. Ying, X. G. Wan, T. Wu, and X. H. Chen, Orbital ordering and fluctuations in a kagome superconductor CsV_3Sb_5 (2021), arXiv:2104.09173 [cond-mat.supr-con].
- [38] J. Luo, Z. Zhao, Y. Z. Zhou, J. Yang, A. F. Fang, H. T. Yang, H. J. Gao, R. Zhou, and G. qing Zheng, Star-of-David pattern charge density wave with additional modulation in the kagome superconductor CsV_3Sb_5 revealed by ^{51}V -NMR and $^{121/123}\text{Sb}$ -NQR (2021), arXiv:2108.10263 [cond-mat.supr-con].
- [39] S. Ni, S. Ma, Y. Zhang, J. Yuan, H. Yang, Z. Lu, N. Wang, J. Sun, Z. Zhao, D. Li, S. Liu, H. Zhang, H. Chen, K. Jin, J. Cheng, L. Yu, F. Zhou, X. Dong, J. Hu, H.-J. Gao, and Z. Zhao, Anisotropic Superconducting Properties of Kagome Metal CsV_3Sb_5 , *Chinese Physics Letters* **38**, 057403 (2021).
- [40] Z. Li, W. H. Jiao, G. H. Cao, and G.-q. Zheng, Charge fluctuations and nodeless superconductivity in quasi-one-dimensional $\text{Ta}_4\text{Pd}_3\text{Te}_{16}$ revealed by ^{125}Te -NMR and ^{181}Ta -NQR, *Phys. Rev. B* **94**, 174511 (2016).